11th Australasian Fluid Mechanics Conference
University of Tasmania, Hobart, Australia
14-18 December 1992

HYPERSONIC IGNITION IN A SCRAMJET

A. PAULL

Department of Mechanical Engineering
University of Queensland
QLD 4072, AUSTRALIA

1. Introduction

Scramjets have been proposed as the main propulsion system for hypersonic reusable aircraft such as the National Aerospace Plane (NASP), Hermes and Sänger. A significant amount of the research into scramjet propulsion systems has been done in Australia using the hypersonic shock tunnels T3 and T4. Unfortunately, the application of this research to an Australian funded project of the size of the above mentioned aircraft is not likely to be realized. However, a scramjet has also been proposed as the propulsion system for a disposable launcher which deploys small payloads into low earth orbit. Such a project could be funded in Australia and furthermore, is a means for Australia to enter the space industry based on technology which is to be used for future launch vehicles. It is such a project that this research into scramjets is directed towards.

2. Experimental Aims

The experiments reported here were undertaken to determine to what extent both hydrogen and ethane would burn at hypersonic conditions. They were required to determine the extent of mixing and at what distance downstream of the injector was combustion complete. It is important to determine this length as too short a combustion chamber will result in inefficient burning, whereas too long a combustion chamber could produce sufficient drag to offset the thrust production.

Results are presented for hypersonic burning of hydrogen and ethane in a rectangular duct. Wall pressures were measured downstream of the injector. From these measurements it is shown that, in contrast to general belief, mixing of hydrogen fuel with air occurs quit rapidly. Furthermore, significant combustion does occur at hypersonic conditions.

Hydrogen was used as a fuel because of its good heat release and therefore good performance in thrust production. The disadvantage with hydrogen is that it is a very bulky fuel. Ethane on the other hand is relatively compact and was believed to have a similar chemistry to that of hydrogen when burnt in air and is thus an attractive fuel.

3. Experimental Apparatus

The experiments reported here were done in the free piston driven hypersonic reflected shock tunnel T4 (Stalker (1966)), figure 1. Typically, the order of the test time in this facility is 1 ms. Data was recorded from each transducer every 2μs.

The scramjet model used in these combustion experiments is shown in figure 2. It a constant area duct into which fuel is injected centrally. The duct is 27 mm high and 54 mm wide and 800mm long. The injector which extends the full width of the duct is 5mm thick. The splitter plate, or upstream edge of the injector, is 76 mm wide and extends 74 mm upstream of the scramjet intake. The splitter plate has been designed so that all shocks and expansions created by the leading edge of the splitter plate are spilled outside the intake to the scramjet.

4. Experimental Results

Two different experiments will be presented. In the first set of experiments the effect on the pressure distribution downstream of the injector produced by injecting different amounts of hydrogen is displayed. In the second set of experiments a comparison between the combustion of hydrogen and ethane is made.

4.1. Equivalence ratio study

In these experiments the measure of the amount of fuel injected into the freestream is made in terms of the equivalence ratio (Φ). A fuel rich mixture has an equivalence ratio greater than one, whereas a fuel lean mixture's equivalence ratio is less than one. The equivalence ratio for hydrogen fuel is equal to 8 times the fuel mass flux through the injector divided by the mass flux of oxygen through the intake.

The mass flow of oxygen into the intake is determined numerically from conditions upstream of the shock tube nozzle using the code NENZF (Lordi et.al (1966)). This program is a one-dimensional nonequilibrum real gas calculations which determines the physical and chemical properties of the test gas at the exit of the nozzle. Input to the calculations are the nozzle contour and the stagnation temperature and pressure.

The stagnation pressure is measured and the stagnation temperature is determined numerically from another real gas calculation performed by the program ESTC (McIntosh (1968)). The inputs for this calculation are the shock tube shock speed and the shock tube filling pressure, both of which are measured.

Fuel was injected at equivalence ratios of 0, 1.1, 1.8 and 4.3. The pressure measurements taken downstream of the injector are displayed in figures 3, 4 and 5. Also displayed in these figures are the effects of injecting similar mass fluxes of fuel into a nitrogen test gas.

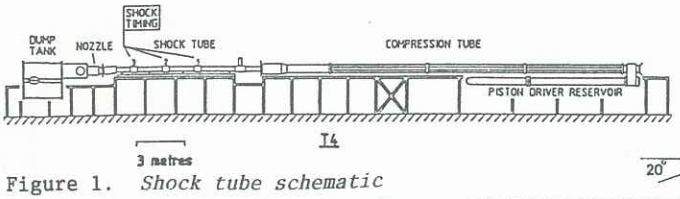

Figure 1. *Shock tube schematic*

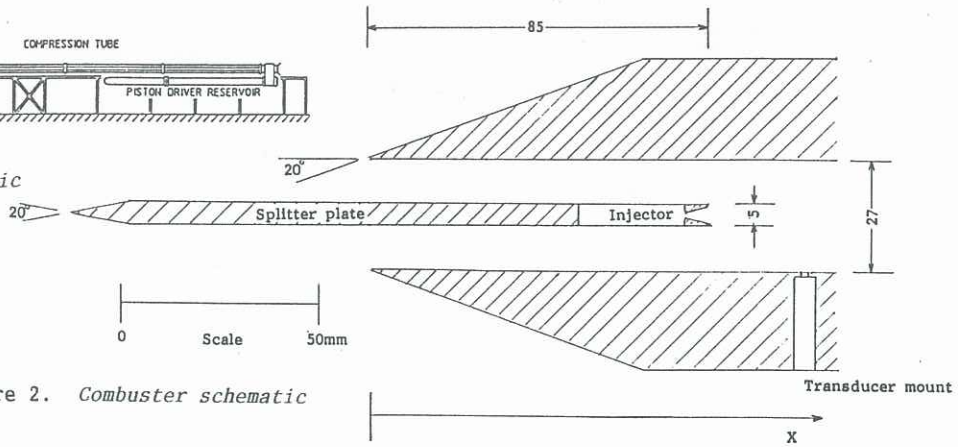

Figure 2. *Combuster schematic*

Due to the different chemistries of nitrogen and air the nitrogen test gas properties at the nozzle exit differ to that of the air's for the same stagnation pressure. The times at which the pressure profiles displayed in figures 3, 4, and 5 have been taken, were chosen so that the static pressure of the nitrogen test gas at the nozzle exit matched that of the air. This can be done as the shock tunnel was run in an under taylored mode and therefore the static pressure was falling with time. Hence, a time could be chosen for which the static pressure was at the required level. The properties of the test gases for each figure are given in table 1.

It can be seen that the pressure rise due to the injection of fuel into air is always greater than that when injected into nitrogen which in turn is greater than that when no fuel is injected. The greater pressure rise produced when fuel is injected into air than that when fuel is injected into nitrogen suggests that the fuel is burning.

Another phenomena which is apparent when the results of figures 3 and 5 are compared is that the pressure rise associated with the injection of fuel at ϕ=4.2 is significantly larger than that for ϕ=1.1. It might be concluded that the injection of more fuel somehow increases the mixing and thus leads to greater combustion and therefore an increase in pressure. However, it is not believed that extra combustion produces the greater pressure rise observed in figure 5.

4.1.1. Mixing analysis

To understand the mechanism which produces the increase in pressure at the higher equivalence ratios the injection of fuel into nitrogen should be considered. Here there is no combustion and yet there is still a significant increase in pressure at the higher equivalence ratio.

If the fuel did not mix with the air then there would be an obvious increase in pressure when more fuel is injected. To obtain an estimate of the pressure rise expected due to the injection of fuel it was assumed that the test gas and the fuel would expand isentropicly from their properties at the exit plane of the injector to one at which their static pressures were matched. If this is done then the final static pressures for ϕ=1.1 and 4.3 are 17.4 and 19.6 kPa, respectively. If fuel were not injected the static pressure would be 16.4 kPa.

There is an added complication in the interpretation of these results. The above pressure rises are superimposed on a pressure rise which occurs in the duct even when fuel is not injected. It is believed that this rise is produced by boundary layer growth. If the test gas was assumed to be isentropicly compressed from 16.4 kPa to the measured value of 24.3 kPa at the end of the duct then this would correspond to a boundary layer thickness of approximately 2.5 mm at the end of the duct. This is not unreasonable when boundary layer theory is considered.

If this boundary layer growth is assumed to remain the same even when the fuel is injected and if it is assumed that the fuel and air do not mix but are compressed by the effect of the boundary layer then it can be shown that the static pressures would rise from 17.4 and 19.6 kPa to 25.9 and 29.0 kPa, respectively for ϕ=1.1 and 4.2. However, as can be seen from figures 3 and 5, this still does not fully explain the increase in pressures which are observed, especially at the higher equivalence ratio.

To include the effects of mixing Morgan et.al.(1990) has assumed that
(a) the fuel and the test gas mix after their static pressures have been matched and
(b) the momentum loss observed in the fuel off results is also lost from the mixed gases.
If these assumptions are made then by enforcing the conservation of mass, momentum and energy it can be shown that the final pressures for a fully mixed nitrogen test gas with the hydrogen fuel would expected to be 27.1 and 35.3 kPa for ϕ=1.1 and 4.23, respectively. It can be seen from figures 3 and 5 that these pressures correspond reasonable well with those measured at the end of the duct. It is concluded that mixing is complete at the latest by the end of the duct.

4.1.2. Combustion analysis

An estimate of the pressure rise due to the effects of combustion are now obtained in the same way that Morgan et.al.(1990) has proposed. When the fuel mixes with air and combustion occurs there is energy released and new products are formed. The effects of combustion are then included by assuming that
(a) the energy released for complete consumption of the available oxygen is added to the energy equation,
(b) the change in specific heat and gas constant due to the combustion products are accounted for

in the final mixture, and
(c) the momentum loss due to the boundary layer growth determined from the fuel off results is the same when combustion occurs.

Although this technique would appear to be a gross simplification of the combustion process, it is a

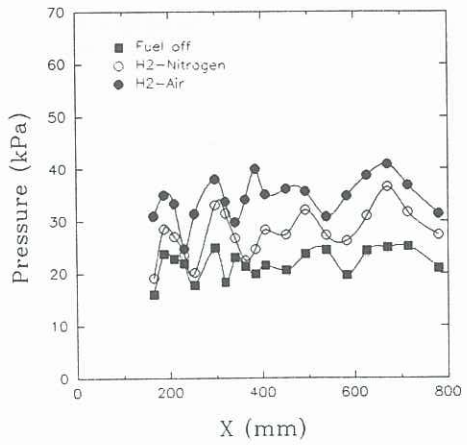

Figure 3. *Pressure vs Distance from intake leading edge ϕ=1.1*

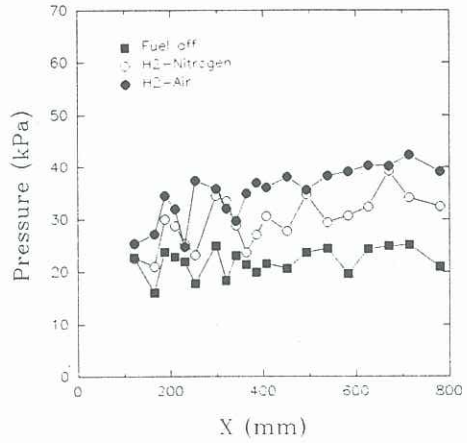

Figure 4. *Pressure vs Distance from intake leading edge ϕ=1.8*

first order approximation to combustion and gives insight into the main mechanisms involved in combustion. If the limitations of this approximations are understood, this type of approximation can be valuable in the understanding of such complex phenomena.

Using the above assumptions it can be shown that the pressures at the exit of the duct could be expected to be 43 kPa and 57 kPa for ϕ=1.1 and 4.2, respectively. From these estimates the experimental results indicate that all oxygen is consumed at both equivalence ratios.

It is concluded that the higher pressures observed at higher equivalence ratios results from more unburnt fuel mixing with the combustion products rather than more complete combustion.

4.1.3. Combustion length

Figure 6 displays the difference between hydrogen injected into air and hydrogen injected into nitrogen at ϕ=1.1, 1.8 and 4.2. These pressure differences have be averaged over spatially adjacent pressure differences to display the trend in pressure differences rather than the actual pressure differences. The actual differences in general undergo large variations between adjacent spatial points. This results from the different intake Mach numbers of the air and nitrogen test

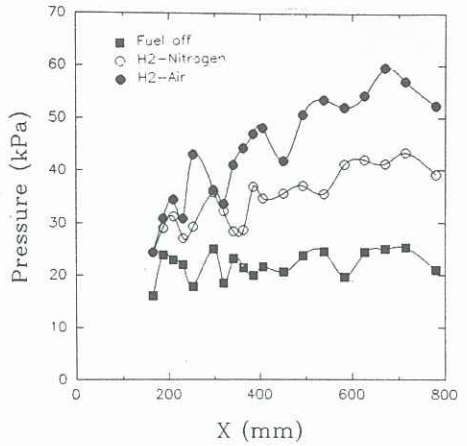

Figure 5. *Pressure vs Distance from intake leading edge ϕ=4.2*

gases producing different Mach wave angles. Thus, the expansion and compressions which are travelling down the duct will be observed at different lateral locations. Spatial averaging over the adjacent points removes this separation. Two observations can be made from figures 6
(a) The pressure rise increases as the equivalence ratio increases and
(b) a significant jump in the pressure can be observed at the wall at x=350 mm downstream of the injector at the higher equivalence ratio.

The first observation was discussed above and results from mixing. The second observation

suggests that either there is a significant increase in mixing at this point or combustion occurs rapidly at this point.

From figure 6 it is seen that for ϕ=1.1 and 1.8 the pressure difference at 200mm is essentially the same as that at the end of the duct. This would indicate that combustion was complete at 200mm (i.e. 115 mm downstream of injection). This does not contradict the induction lengths predicted by Nettleton (1992) which indicate that a stoichometric mixture of hydrogen and air has an induction length of approximately 50mm for the intake conditions of these experiments.

If it is assumed that combustion also takes place at the same rate for ϕ=4.2 as ϕ=1.1 and ϕ=1.8 (as is indicated in figure 6 for x<300) then the large jump in pressure observed at the higher equivalence ratio at x=350 is probable caused by significant mixing at this point. It can be seen from figure 5 that at this point there is a shock and expansion system which is propagating through the mixture at this point. It is possible that this system enhances mixing and is thus possibly a useful mechanism.

4.2. Ethane-Hydrogen comparison

The combustion of ethane was compared with that of hydrogen at the stagnation enthalpies of 8.6 and 11.6 MJ/kg. Table 1 lists the flow parameters.

It can be seen that at the higher stagnation enthalpy the pressure rise produced by ethane and hydrogen were almost indistinguishable. Whereas, at the lower enthalpy the net increase in pressure produced by the ethane was approximately half that produced by the hydrogen. If the duct were longer it is not clear whether or not this would have been the case. Ethane may be mixing limited.

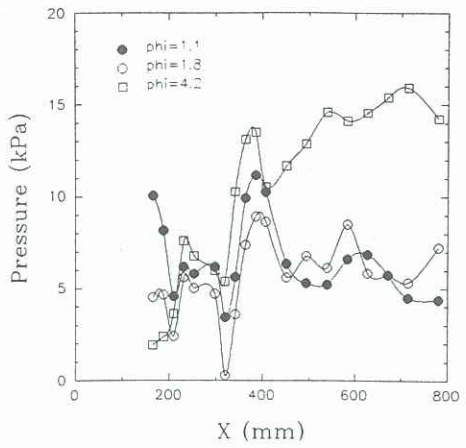

Figure 6. *Pressure difference between fuel into air and into nitrogen vs Distance from the intake leading edge for different equivalent ratios.*

Not-with-standing the pressure rise associated with ethane, even at the higher enthalpies, would indicated that ethane is not as an efficient fuel as hydrogen if efficiency is based on specific impulse. This follows because for the same equivalence ratio the mass of ethane is 15/7 times that of hydrogen. Hence, to produce the same thrust per unit mass of fuel the pressure rise produced by the ethane would have to be 15/7 times that produced by hydrogen.

However, it should be understood that efficiency based upon specific impulse is not necessarily applicable when comparing different fuels for flight vehicles. This is because more dense fuels require smaller fuel tanks and therefore less drag will be produced by the vehicle which runs on higher density fuels. Hence, dense fuels with smaller specific impulses than less dense fuels may in fact be more efficient overall.

Conclusions

At the enthalpy of 15 MJ/kg hydrogen can be made to burn effectively. The burning process does appear to be limited by mixing, but the experimental results indicate that it is not a server limitation. In practical terms these mixing limitations would not pose a problem to the design of a workable engine.

The induction process for the combustion of hydrogen predicted by Nettleton (1992) would appear to be consistent, at least to an order of magnitude, to that measured.

Ethane fuel produces pressure rise which is at most equal to that produced by hydrogen. Hence, if efficiency is based upon specific impulse it is expected that ethane would not be as an efficient fuel as hydrogen.

Acknowledgements

This work was done under grants supplied by The Australian Research Council and NASA.

Bibliography

Lordi, J.A., Mates, R.E. and Moselle, J.R. 1966 Comp. prog. for numerical soln. of nonequilibrum expansion of reacting gas mixtures. NASA CR-472

McIntosh, M.K. 1968 Computer. program for the numerical calculation of frozen and equilibrium conditions in shock tunnels. Dept. of Phys. ANU

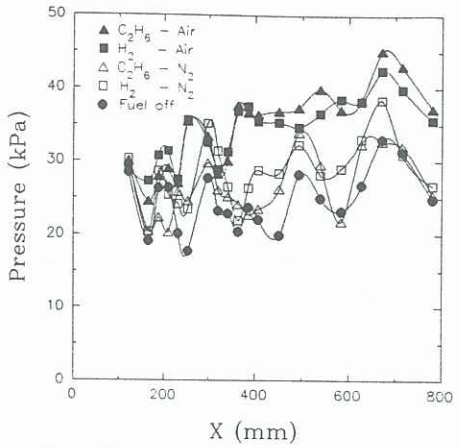

Figure 7. *Pressure vs Distance for hydrogen and ethane fuels. Stag. enthalpy nominally 12MJ/kg*

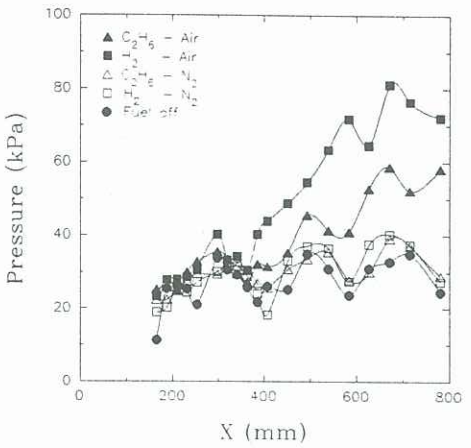

Figure 8. *Pressure vs Distance for hydrogen and ethane fuels. Stag. enthalpy nominally 9MJ/kg*

Morgan R.G. Bakos, R.J. and Tamagno, J. 1990 Bulk parameter analysis of hypersonic combustion experiments GASL TR321

Nettleton M. 1992 On the existance of real standing detonations in scramjet ducts AFMC 1992

Stalker, R.J. 1966 The free piston shock tunnel. Aeronaut. Q. V17 pp351-370.

Fig.	gas	Enth. MJ/kg	Press. kPa	Vel. m/s	Den. kg/m	M	ϕ	Fuel
3	Air	14.7	20.3	4608	.032	5.1	1.1	H2
3	N2	15.5	20.7	4926	.032	5.4	1.2	H2
3,4,5	Air	14.9	20.3	4627	.032	5.1	0.0	
4	Air	15.0	19.0	4648	.030	5.1	1.8	H2
4	N2	15.6	19.0	4929	.029	5.4	1.7	H2
5	Air	14.7	20.3	4634	.032	5.1	4.2	H2
5	N2	15.4	20.5	4914	.032	5.4	4.4	H2
7	Air	11.7	18.3	4186	.032	5.2	1.6	H2,C2H6
7	Air	11.7	18.3	4186	.032	5.2	0.0	
7	N2	12.6	18.3	4556	.036	5.6	1.8	H2,C2H6
8	Air	8.64	18.9	3718	.054	5.5	1.9	H2,C2H6
8	Air	8.64	18.9	3718	.054	5.5	0.0	
8	N2	9.13	19.1	3952	.055	5.8	1.7	H2,C2H6

Table 1. *Test conditions.*